

## Comparative lipid analysis and structure of detergent-resistant membrane raft fractions isolated from human and ruminant erythrocytes

Kamen S. Koumanov<sup>a</sup>, Cedric Tessier<sup>b</sup>, Albena B. Momchilova<sup>a</sup>, Dominique Rainteau<sup>b</sup>, Claude Wolf<sup>b</sup>, Peter J. Quinn<sup>c,\*</sup>

<sup>a</sup> Institute of Biophysics, Bulgarian Academy of Sciences, 1113 Sofia, Bulgaria

<sup>b</sup> Faculté de Médecine Saint Antoine, Université Paris 6, INSERM U538, 27 rue Chaligny, Paris 75012, France

<sup>c</sup> Department of Life Sciences, King's College London, 150 Stamford Street, London SE1 9NN, UK

Received 10 September 2004, and in revised form 19 October 2004

Available online 25 November 2004

### Abstract

The lipid composition and structure of detergent-resistant membrane rafts from human, goat, and sheep erythrocytes is investigated. While the sphingomyelin:cholesterol ratio varied from about 1:5 in human to 1:1 in sheep erythrocytes a ratio of 1:1 was found in all raft preparations insoluble in Triton X-100 at 4 °C. Excess cholesterol is excluded from rafts and saturated molecular species of sphingomyelin assayed by gas chromatography–mass spectrometry determines the solubility of cholesterol in the detergent. Freeze-fracture electron microscopy shows that vesicles and multilamellar structures formed by membrane rafts have undergone considerable rearrangement from the original membrane. No membrane-associated particles are observed. Synchrotron X-ray diffraction studies showed that *d* spacings of vesicle preparations of rafts cannot be distinguished from ghost membranes from which they are derived. Dispersions of total polar lipid extracts of sheep rafts show phase separation of inverted hexagonal structure upon heating and this phase coexists with multilamellar structures at 37 °C.

© 2004 Elsevier Inc. All rights reserved.

**Keywords:** Erythrocyte raft lipids; Raft structure; Lipid composition of membrane rafts; Detergent-resistant membranes

The asymmetric distribution of various components within biological membranes is now established into the dogma of membrane structure. An example is the creation of various intercellular membrane junctions and coated pits. In these examples interactions of membrane-associated proteins are believed to be responsible for creating specialized domains. In addition to the protein-driven alteration of membrane lipids, attention has been recently directed to the primary role of lipid–lipid interactions in the creation of lateral domains. Lateral lipid phase separation in biological membranes at low temperatures is well known. The phase separation in this

case is driven by transition of high melting point lipids into gel phase and zone refining effects leading to the exclusion of fluid domains [1]. A subtle form of lateral phase separation occurs in membranes containing high proportions of cholesterol, notably the plasma membrane, in which saturated lipids otherwise existing in gel phase associate into complexes with the sterol to form a liquid-ordered phase after zone refining [2]. The liquid-ordered phase is typified by a relatively high ordering of the extended acyl chains but is distinguished from a gel phase by a rapid lateral mobility of the lipid molecules ( $2\text{--}5 \times 10^{-12} \text{ m}^2/\text{s}$ ) [3]. Domains (or microdomains) of liquid-ordered phase, referred to as rafts, are expected to occur in biological membranes containing appropriate amounts of sphingolipids and cholesterol.

\* Corresponding author. Fax: +44 2078484500.

E-mail address: [p.quinn@kcl.ac.uk](mailto:p.quinn@kcl.ac.uk) (P.J. Quinn).

The factors responsible for creating raft domains are believed to be interactions between lipids [4,5] but interactions between lipids and elements of the cytoskeleton [6–10] may also be involved. Isolation of liquid-ordered domains from biological membranes has been achieved operationally by differential solubility in detergents such as Triton X-100. Fractions resisting solubilization by detergent yield the fraction referred to as detergent-resistant membranes (DRM).<sup>1</sup> This is assumed to represent the raft domains preexisting in the membrane. However, the use of detergents to fractionate membranes is problematic in that it is uncertain as to whether all the original associations, including lipid–lipid and lipid–protein associations, survive exposure to detergent. For this reason the chemical composition of membrane domains and the factors assumed to govern raft formation in membranes has been questioned [11,12]. Detergent-resistant membrane fractions have been commonly prepared from a variety of membranes including plasma [13–16] and Golgi membranes [17]. Analysis of DRMs has confirmed that all are invariably enriched in sphingolipids and cholesterol [13,18,19]. The proteins associated with the intact membranes from which rafts are prepared are distinct from those solubilized by detergent. Lipidation is believed to explain the particular concentration of glycerylphosphoinositol-anchored and acylated-proteins in rafts [20–22]. Because the lipid and protein composition differs from whole membrane specialized raft domains are assumed to be involved in vivo in particular membrane functions such as membrane budding [23], fusion [24,25], signal transduction [21,26–30], protein sorting and trafficking [5,15,16,31].

Characterization of liquid-ordered phase domains in biological membranes has proven to be difficult to demonstrate. Nevertheless, estimates using model dependent spectroscopic methods have been made of the size of membrane raft domains that vary from associations of 20–30 molecules [32] to domains extending to hundreds of nm [33,34]. The concept of membrane rafts relies mainly on results of studies using molecular probe methods and model membrane lipid mixtures. There are few reports of raft structure using electron microscopic or X-ray diffraction techniques.

The present study was undertaken to examine the composition and structure of DRMs prepared from erythrocyte membranes. While X-ray diffraction studies have been performed on dispersions of lipid extracts of DRMs [35] no examination of the original membrane fractions including proteins has yet been reported. The

present results reveal that biophysical data collected with ruminant DRM are only partially in line with what is expected for liquid-ordered domains of similar lipid composition. The results indicate clear differences between the structure and phase behaviour of dispersions of lipids extracted from DRM preparations and the intact rafts which suggests that the presence of raft proteins and/or retention of an arrangement of components that differ from random dispersions of lipids may be responsible.

## Materials and methods

### *Erythrocyte ghost preparation*

Human and ruminant erythrocytes were isolated from fresh citrated blood by procedures described previously [36]. Briefly, whole blood was centrifuged for 10 min at 100g. The erythrocytes were harvested and washed three times with 5 vol. of a buffer consisting of 150 mM NaCl, 5 mM sodium phosphate (pH 8.0) (PBS) and lysed in 40 vol. of 5 mM sodium phosphate (pH 8.0). The resulting membrane ghosts were collected by centrifugation for 20 min at 22,000g and washed up to four times with lysing buffer until ‘white ghosts’ were obtained.

### *Preparation of detergent-resistant membrane fractions*

Erythrocyte ghosts were resuspended in buffer consisting of 0.25 M sucrose, 150 mM NaCl, 1 mM EDTA, and 20 mM Tris–HCl buffer (pH 7.6) containing 1% (v/v) Triton X-100 at 4 °C and dispersed by 10 passages through a 21 gauge needle. The suspension was diluted with an equal volume of 80% (w/v) sucrose. Four millilitre of this detergent-treated membrane suspension was seated in a centrifuge tube covered by successive layers of 30% (w/v) sucrose (4 ml) and 5% (w/v) sucrose (3.5 ml). The discontinuous density gradients were centrifuged for 18 h at 38,000g in a SW41 Beckman rotor. The material layered at the 5/30% (w/v) sucrose interface was designated as DRMs and harvested for further analysis.

### *Lipid extraction and phospholipid analysis*

Extraction of polar lipids was performed by the method of Bligh and Dyer [37]. Samples of the extracts were subjected to analysis by thin-layer chromatography on silica gel plates (Merck) developed with a solvent system consisting of chloroform/methanol/acetic acid/H<sub>2</sub>O (60:30:8:4 v/v). The phospholipid spots were scraped off the plate and extracted with chloroform/methanol, 2:1 (v/v). The glycerophospholipids in the fractions were saponified in 0.5 N KOH methanol at 60 °C for 15 min and the fatty acids released from the ester bonding were methylated using boron trifluoride:methanol complex

<sup>1</sup> Abbreviations used: SM, sphingomyelin; PC, phosphatidylcholine; PS, phosphatidylserine; PI, phosphatidylinositol; PE, phosphatidylethanolamine; chol, cholesterol; DRM, detergent-resistant membrane; SAT, saturated fatty acids; MONO, monoenoic fatty acids; PUFA, polyunsaturated fatty acids; SAXS, small-angle X-ray scattering; WAXS, wide-angle X-ray scattering; Lo-phase, liquid-ordered bilayer phase.

reagent for 15 min at 60 °C. Amidated fatty acids of sphingolipids were cleaved by acetonitrile:HCl (0.5 N hydrochloric acid in acetonitrile/water, 9/1, v/v) for 4 h at 70 °C and the fatty acids methylated by diazomethane.

#### *Fatty acid analysis*

The methylated fatty acids were separated by gas chromatography on a highly polar capillary column coated with Supelcowax-10-bound phase (i.d. 0.32 mm, length 30 m, film thickness 0.25 µm; (Supelco, Bellefonte, PA)) fitted in a Hewlett-Packard (Palo Alto, CA) 5890 Series II gas chromatograph. Fatty acids were detected with picomolar sensitivity by mass spectrometry (Nermag 10-10C, Quad-Service, Poissy, France) in the chemical ionization mode with ammonia ( $10^4$  Pa) as the reagent gas. The positive quasimolecular ions [M + 18] were selectively monitored and time integrated. Quantitation was achieved by normalization with an internal standard of heptadecanoic methyl ester and the response factors for the various fatty acids were calculated with methyl ester calibrators.

#### *Cholesterol determination*

The non-esterified cholesterol (Chol) content of ghost and DRM fractions was assayed by gas chromatography–mass spectrometry of the trimethylsilyl ether [38] (CHROMPACK, Middelburg, The Netherlands). The cholesterol derivative was separated by gas chromatography on a medium polarity RTX-65 capillary column (0.32 mm internal diameter; length 30 m; film thickness 0.25 µm). Using electron impact mode at 70 eV the positive fragment ion ( $m/z = 329$ ) was used to quantitate Chol content after normalization with an internal standard of epicoprostanol. Calibration was achieved by a weighted standard of Chol.

#### *Freeze-fracture electron microscopy*

Detergent-resistant membrane fractions and dispersed lipid extracts were sandwiched between two copper sample mounts (Balzers Union 120557/1205 JT) and equilibrated at 20 °C using a thermally stable gas flow for 3 min prior to thermal quenching. Samples were thermally quenched in a liquid nitrogen jet freezer. Fracturing and replication were performed at –150 °C using a Polaron B7500 freeze-fracture device. Replicas were cleaned in a solvent consisting of chloroform:methanol (2:1, by volume) before examination in a Joel JEM100CX electron microscope.

#### *Synchrotron X-ray diffraction*

DRM were oriented by centrifugation (100,000g, 1 h) and the pellet deposited on a small aluminium foil was

transferred from the tube to the sample cell sandwiched between a pair of thin mica sheets. The cell was clamped to a thermostated stage (Linkam Scientific Instruments, UK). X-ray scattering intensities at small-angles (SAXS) were recorded using a multiwire quadrant detector at a distance of 2 m from the sample. Wide-angle scattering (WAXS) was recorded using a curved INEL (INstrument Electronique, France) detector at a distance from the sample of 0.40 m. Experimental data were analysed using the OTOKO software kindly provided by M. Koch [39]. Scattering intensities were corrected for channel detector response using homogeneous irradiation from a  $^{55}\text{Fe}$  source. Spatial calibrations were obtained using higher-orders of reflection from wet rat-tail collagen ( $d = 67$  nm) [40]. The reciprocal spacing are given as  $S = 1/d = 2 \sin(\theta)/\lambda$ , where  $d$ ,  $\lambda$ , and  $\theta$  are repeat distance, X-ray wavelength and the diffraction angle, respectively. Synchrotron X-ray diffraction experiments were performed using a monochromatic (0.15405 nm) focused X-ray beam at station 8.2 or 16.1 of Daresbury Synchrotron Radiation Laboratory (Warrington, UK). A web site describes in details the facility available at station 16.1 (<http://www.srs.ac.uk/srs/stations/station16.1.htm>).

## **Results**

#### *Lipid analyses*

An analysis of human, sheep, and goat erythrocyte membranes and respective DRM fractions were undertaken to quantitate the lipid classes populating the liquid-ordered phase resistant to detergent solubilization. The distribution of major lipid classes in ghosts and DRM fractions is presented in Table 1. Deviation about mean values is small confirming that the detergent treatment results in reproducible DRM fractions ( $n \geq 3$  independent preparations). A noteworthy feature of the composition is the relatively high proportion of SM in ruminant erythrocyte ghosts as compared with human which is the result of a substitution of PC by SM. The ratio SM:PC in the erythrocyte membrane of different animal species varies widely from 0.8 to 0.7 in human to 10 to 13 in goat and bovine [41] and 310 in sheep erythrocytes. Since SM is the dominant phospholipid of the DRM fraction the proportion of the ghost membrane remaining insoluble in detergent is greater in ruminant compared with human erythrocyte ghosts. Thus, human DRM fractions collected after Triton X-100 treatment represent only 5% of the total lipid content of the membrane whereas this amounts to 27% in goat and 35% in sheep. The ratio SM:cholesterol in DRM fractions prepared from the various animal species is of particular interest with regard to previous experimental studies where a defined stoichiometry is believed to be required to form SM-cholesterol com-

Table 1

The molar proportions of the major lipids of human, goat and sheep erythrocyte ghosts and DRM fractions derived therefrom

Phospholipids	Human		Goat		Sheep	
	Ghosts	DRM	Ghosts	DRM	Ghosts	DRM
SM	12.12 ± 2.14	44.51 ± 4.54	25.85 ± 1.25	32.27 ± 2.84	41.59 ± 3.25	43.63 ± 4.86
PC	16.70 ± 1.58	4.62 ± 0.32	2.05 ± 0.14	4.54 ± 0.38	0.13 ± 0.05	0.30 ± 0.06
PS/PI	6.40 ± 0.45	8.72 ± 0.81	14.04 ± 2.01	15.58 ± 1.85	5.06 ± 0.36	6.47 ± 0.39
PE	10.78 ± 0.87	2.22 ± 0.35	9.71 ± 0.74	16.55 ± 1.11	14.00 ± 1.69	4.16 ± 0.56
Chol	54.00 ± 3.41	39.93 ± 4.11	48.35 ± 5.09	31.06 ± 2.89	39.23 ± 4.45	45.44 ± 3.85
	100	100	100	100	100	100

plexes in the liquid-ordered phase. The present results show that SM:cholesterol varies in a narrow range from 0.97 (sheep) to 1.1 (human) and is independent of the total cholesterol content of the respective membranes from which the DRMs were prepared. The composition of sheep DRM bears a remarkable resemblance to the composition of the intact ghost membrane except that PE is significantly lower. In the goat and particularly the human DRM it is clear that most of the cholesterol of the ghost membrane is excluded from the DRM fraction and it is the sphingomyelin that determines the amount of cholesterol solubilized by Triton. This suggests that cholesterol resists solubilization only so long as it is associated with SM. SM along with other sphingolipids is known to be resistant to solubilization because the hydrocarbon chains are relatively longer and more saturated which favours their association with cholesterol. The condensed state of the ordered phase formed by SM and cholesterol is said to resist intercalation of detergent molecules.

Unlike human ghosts where PC is the most abundant phospholipid (about 17 mol%) it occurs only as a minor fraction in ruminants. Aminoglycerophospholipids, PE and PS, are the prominent glycerophospholipids of goat and sheep erythrocyte ghosts. In ruminant DRMs PE/PS ratio is quite similar but it differs widely in the whole erythrocyte membranes in which the acidic phospholipid fraction of goat erythrocytes is particularly conspicuous. PE in DRMs varies amongst animal species independently of whole membranes while PS is correlated with proportions found in the original membranes. A comparison between the major lipids of erythrocytes and DRMs of human and goat membranes, typical of ruminants, is presented graphically in Fig. 1.

To investigate the reason for detergent insolubility of SM the fatty acid composition of the phospholipid recovered in DRM fractions was determined and the molecular species compared with SM found in the respective ghost membranes from which DRMs were prepared. The amide-bound fatty acids of SM purified from human and ruminant erythrocyte ghosts and corresponding DRM fractions are shown in Table 2. In all cases the saturated molecular species of SM are more

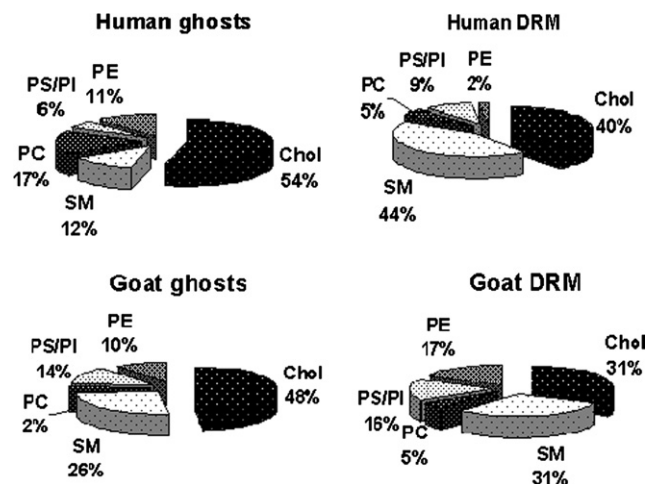


Fig. 1. Lipid composition of human and goat erythrocyte membranes and corresponding DRM fractions.

abundant in DRM fractions than in intact ghosts. The dominance of saturated molecular species occurs at the expense of monoenoic fatty acids which are more abundant in the original membranes. Ruminant erythrocytes, however, contain much higher proportions of 24:1 than 24:0 compared with human erythrocytes and this is reflected in the lower ratios of saturated:monounsaturated fatty acids amide bonded to SM. Human DRMs show a threefold enrichment of C22:0 and C24:0 SM but only traces of C24:1. Similarly the goat and sheep DRM fractions are enriched in C16:0 SM but depleted in C18:1 and C24:1 species relative to the original membranes.

#### Electron microscopic studies

The structure of DRM preparations from human and goat erythrocytes was examined by freeze-fracture electron microscopy and compared with intact erythrocyte ghost membrane (Fig. 2). A typical freeze-fracture image of an etched human erythrocyte membrane viewed from the outside aspect of the cell is shown in Fig. 2A. The P-face shows characteristic distribution of membrane-associated particles and the etched surface of the cell shows a texture reflecting the arrangement of the underlying particles. Replicas from human DRM (Fig. 2B)



Table 2

Fatty acid composition of amide-linked substituents to sphingomyelin in human, goat, and sheep erythrocyte ghosts and DRM fractions

Fatty acid	Human		Goat		Sheep	
	Ghosts	DRM	Ghosts	DRM	Ghosts	DRM
	C16:0	41.45 ± 5.68	8.63 ± 0.74	27.94 ± 1.35	44.26 ± 5.21	35.46 ± 3.65
C18:0	6.25 ± 0.74	6.36 ± 0.66	3.27 ± 0.42	3.44 ± 0.29	1.40 ± 0.18	5.29 ± 0.65
C18:1	1.15 ± 0.21	1.49 ± 0.21	7.80 ± 0.62	0.86 ± 0.09	0.26 ± 0.15	1.29 ± 0.21
C18:2	0.10 ± 0.01	0.18 ± 0.03	0.79 ± 0.09	0.15 ± 0.01	0.07 ± 0.01	0.16 ± 0.02
C20:0	0.70 ± 0.00	2.22 ± 0.03	0.07 ± 0.01	0.06 ± 0.00	0.08 ± 0.01	0.11 ± 0.01
C22:0	5.78 ± 0.48	14.72 ± 2.02	0.76 ± 0.09	0.65 ± 0.05	2.14 ± 0.31	0.77 ± 0.08
C24:0	20.02 ± 2.35	62.10 ± 5.69	1.59 ± 0.10	1.92 ± 0.18	6.15 ± 0.75	1.41 ± 0.11
C24:1	24.02 ± 1.87	1.47 ± 0.19	55.58 ± 4.85	47.07 ± 6.25	51.39 ± 6.32	15.85 ± 1.31
C26:0	0.33 ± 0.04	2.78 ± 0.21	0.11 ± 0.02	0.09 ± 0.01	0.34 ± 0.03	0.04 ± 0.01
C26:1	0.19 ± 0.01	0.05 ± 0.00	2.10 ± 0.18	1.52 ± 0.28	2.70 ± 0.31	0.50 ± 0.06
Total	100	100	100	100	100	100
SAT	74.54	96.81	33.74	50.41	45.57	82.20
MONO	25.36	3.01	65.48	49.44	54.35	17.64
PUFA	0.10	0.18	0.79	0.15	0.07	0.16

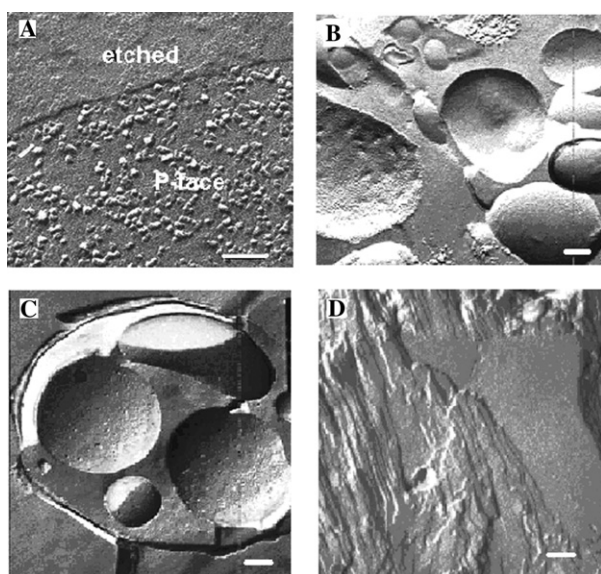


Fig. 2. Electron micrographs of freeze-fracture replicas of (A) etched human erythrocyte membrane and DRM fractions prepared from (B) human (C) goat erythrocyte membranes. (D) Lipid extract from goat DRM dispersed in aqueous medium. Bars = 100 nm.

show vesicles some of which contain more than one layer. The fracture faces of both the inner and outer fracture planes of the vesicles are typically smooth and devoid of the membrane-associated particles of the type observed in the intact erythrocyte membrane. Occasionally, the fracture plane within the vesicle reveals a roughened texture on the surface but the appearance is clearly distinct from that of the intact membrane. Electron micrographs of replicas prepared from suspensions of DRM from goat (Fig. 2C) are similar to those of human but the fracture planes revealing the inner monolayers show a low density of small membrane-associ-

ated particles; the outer monolayers tend to be smooth in appearance. The results show that the original membrane undergoes considerable reorganization as a result of exposure to detergent in that the original ghost membrane is disrupted so that vesicles become trapped within larger vesicles and multilamellar structures are observed. Whether or not asymmetric distribution of constituents across the membrane is preserved is conjectural but clearly the constituents responsible for forming membrane-associated particles are either rearranged or excluded from the membrane. Further studies were undertaken to compare the appearance of the DRM fractions with the structure of aqueous dispersions of the lipid extracts derived from the DRM. An electron micrograph of a dispersion of total polar lipids extracted from a goat erythrocyte DRM preparation is shown in Fig. 2D. This shows that at a quench temperature of 20 °C a multilamellar phase dominates the structure making it accessible to small-angle X-ray diffraction analysis.

#### Synchrotron X-ray diffraction measurements

The structure of DRM fractions from human and ruminant erythrocytes was examined by synchrotron X-ray diffraction methods. Small-angle X-ray diffraction patterns recorded from suspensions of DRMs from erythrocyte ghosts of human, sheep, and goat are presented in Fig. 3. All membranes show sharp peaks in the region corresponding to repeat spacings of 5–6 nm. Examination of the change in the position of these peaks as a function of temperature (data not shown) indicates that the peaks about 5.1 nm arise from a different arrangement of the membranes from those centred at about 6.1 nm. Higher-order reflections are observed at a spacing of about 3 nm when the reflection at 6.1 nm predominates suggesting that this peak is a reflection

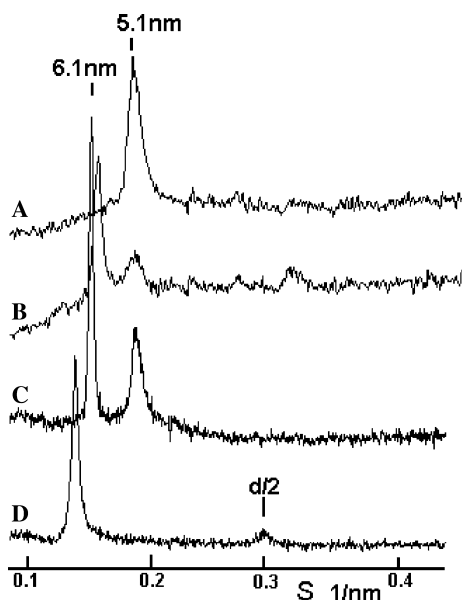


Fig. 3. Small-angle X-ray scattering intensity patterns recorded from suspensions of DRMs prepared from (A) human, (B) sheep, and (C) goat erythrocyte ghosts. (D) Goat DRMs suspended in buffer containing 1% Triton X-100. All patterns were recorded at 37 °C.

from stacked arrays of membrane. The peak at about 5.1 nm has no corresponding higher-order reflections but we assign this peak to unoriented vesicles on the basis of the reciprocal changes in intensities of the two peaks as a function of temperature (data not shown). The addition of Triton X-100 to the suspension of goat DRM causes the vesicles to align in multilamellar stacks which have a repeat spacing somewhat greater (6.5 nm) than the stacked arrays of DRM preparations and the stacking order is more regular as evidenced by the prominent reflection at  $d/2$ . This suggests that the detergent influences the hydration forces between the bilayers but does not destroy the bilayer structure even at temperatures greater than 4 °C. The wide-angle region of the scattering patterns show broad scattering bands centered at 0.455 nm indicative of a disordered hydrocarbon phase.

The thermotropic phase behaviour of dispersions of total lipid extracts prepared from sheep DRMs was investigated to determine the role of the non-lipid components in the structure and stability of the rafts. Small-angle X-ray scattering intensity patterns recorded at 10, 37, and 50 °C during a heating scan are presented in Fig. 4. A multilamellar phase indexed by two-orders of reflection is seen at 10 °C. The appearance of a non-lamellar phase is observed when the temperature exceeds about 30 °C and is indexed by higher-order reflections consistent with hexagonal-II phase ( $1 = d/1$ ;  $2 = d/\sqrt{3}$ ;  $3 = d/\sqrt{4}$ ). The hexagonal-II phase ( $d$  spacing 6.1 nm) coexists with the multilamellar phase ( $d$  spacing 5.7 nm) on heating up to 50 °C and is completely reversed on cooling below 30 °C.

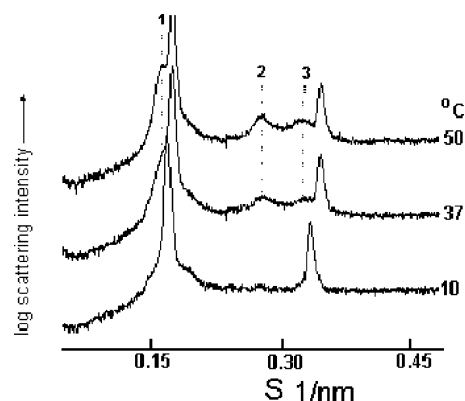


Fig. 4. Small-angle X-ray scattering intensity patterns recorded from an aqueous dispersion of total polar lipids from sheep DRM at designated temperatures during a heating scan. The data are plotted on a logarithmic scale to emphasize the weakly scattering peaks. The orders of reflection from the hexagonal-II phase are indicated.

## Discussion

The composition of the DRMs from different species is remarkably similar despite considerable differences in the composition of the erythrocyte membranes from which they were prepared. Unlike human ghosts in which PC dominates the major phospholipid composition more than half of ruminant phospholipid is SM, also a choline-containing phospholipid (Table 1). This feature appears to be characteristic of ruminants since a similar composition was also observed for bovine erythrocytes [42]. The high content of SM is correlated with the reduction of PC while other phospholipids vary less. This is consistent with the presence of a highly active PC-specific phospholipase-A<sub>2</sub> in bovine ghosts [42] and which is also found in goat and sheep erythrocytes (Koumanov, unpublished). Another significant difference between human and ruminant erythrocyte lipids was the fatty acid composition characterizing the different molecular species of SM. SM usually contains high levels of nervonic acid (C24:1N-9) as the most abundant unsaturated fatty acid of the membrane. This holds for human as well as in goat and sheep ghosts. However, in ruminant erythrocytes the level was twice that of human erythrocytes. The reason why the proportion of nervonic acid in goat DRM is particularly high is unclear. Due to the higher SM content ruminant DRM fractions represent about 30% of the total ghost lipid but only 5% in human. This is consistent with the proportion of SM and cholesterol in the ghost membranes and presumably reflects the extent of ordered lipid domains (Lo-phase) in the intact membrane that resists solubilization by Triton.

In both human and ruminant DRM preparations a consistent finding is a ratio SM:Chol of about 1. Whether a complex of this stoichiometry is present in the DRMs cannot be concluded from the available evidence because

other (glycero)phospholipids are also present in the DRM fraction. The failure to detect sharp WAXS reflections indicative of gel phases that would be predicted to form at temperatures below 30 °C is consistent with interaction of saturated molecular species of SM with cholesterol. A ratio lower than equimolar for SM:cholesterol could be expected for Lo phase in DRM if part of cholesterol is to partition with glycerophospholipids. Indeed, the low solubility of cholesterol in aminophospholipids PE and PS [43] which are found associated with DRM implies that the ratio SM:cholesterol is probably close to the value of 1. As pointed out in recent reviews [44,45] the stoichiometry for such a SM:cholesterol complex is dependent on the physical state of the system such as lateral pressure and temperature.

One notable feature concerning the cholesterol content of DRMs is that the mixture is close to crystallization of cholesterol within the bilayer. In sheep DRMs cholesterol microcrystals have been observed when temperatures exceed 45 °C, a condition that is presumed to decrease the association of cholesterol with the least saturated molecular species of SM. The phase separation is reversible on cooling. This observation implies that DRMs are able to maintain their cholesterol content via cholesterol separation of microcrystals. Such a possibility has already been observed in previous studies of biological membranes [46].

While the phospholipid and fatty acid composition of erythrocyte ghost membranes differ significantly the DRMs are invariably enriched with saturated molecular species of SM. Saturated molecular species of SM or PC associated with cholesterol are known to form Lo-phase on the basis of model membrane studies [47,48]. Indeed, the compact nature of the Lo phase and resistance to detergent solubilization is believed to be due to a reduction of *gauche* rotational isomers of the acyl chains of the high melting temperature molecular species of SM in van der Waals contact with the  $\alpha$ -face of the cholesterol ring structures [49].

It is important to recognize that the composition of DRMs is determined by the detergent and the procedures used to isolate them. Thus, detergents such as Triton X-100, Tween, Brij58, and Lubrol differ markedly in their ability to selectively solubilize membrane proteins and to promote enrichment in sphingomyelin and cholesterol at the expense of glycerophospholipids and saturated compared with unsaturated choline phosphatides [50]. A comparison of the lipid composition of rafts prepared using a non-detergent method [50] with parent membranes isolated from a human epidermoid cell line, nevertheless showed a threefold enrichment of cholesterol in the raft fraction [51]. The DRM preparations from erythrocyte ghost membranes are in the form of vesicles as seen from the electron microscopic evidence. The vesicles are of variable size and configuration with closed vesicles enveloped by larger vesicles. This indi-

cates that considerable disruption occurs during exposure of the ghost membrane to the detergent. The important question is how extensive is this disruption? One obvious feature of all the DRM preparations is the absence of membrane-associated particles from the inner fracture plane. This is consistent with the presence of an ordered structure of the hydrocarbon chains from which components that comprise these membrane-associated particles are often excluded [52]. The question of whether exposure of erythrocyte ghosts to Triton results in reorganization of the membrane into fragments of the original membrane which form stable vesicles of raft membrane or whether the detergent causes the dissociation of membrane components and their reassembly into DRMs can be addressed from the X-ray diffraction results. An indication of the structure and stability of DRMs can be deduced from the effect of adding Triton X-100 to the DRM preparation. The presence of the detergent changed the macroscopic order of vesicle suspensions and caused the membranes to aggregate into multilamellar arrays. The arrays were stable over the temperature range 4–45 °C consistent with the predicted effect of Triton in concentrations used to prepare the DRMs [53]. The only detectable effect on the structure was an increase in *d* spacing of the multilamellar array by 0.2 nm.

The stability of the rafts can be judged from a comparison of the thermotropic behaviour of the raft preparation from sheep erythrocytes with that of dispersions of total polar lipid extracts of the rafts. The X-ray scattering intensity patterns recorded from the raft preparation remains unchanged during heating up to 40 °C. By contrast, an hexagonal-II structure begins to phase separate from the lamellar structure at about 30 °C during the heating scan. Clearly the non-bilayer forming lipids present in the raft membrane are constrained into a bilayer either by their particular configuration in the raft membrane or their interaction with the non-lipid components of the raft. The relative proportion of the scattering arising from the hexagonal-II and lamellar structures suggests that the particular arrangement of the lipids is a significant factor. Since there is also no evidence of lipid phase separation in the erythrocyte ghost membranes at temperatures at least up to 40 °C the inference is that the lipid configuration in the ghost membrane is preserved in the raft.

One of the distinguishing features of membrane rafts is said to be that the hydrocarbon thickness is greater than non-raft domains of the membrane and that this difference is exploited in sorting intrinsic membrane proteins [5,54]. An X-ray diffraction study of model systems in which the hydrocarbon thickness of lipid mixtures which resist solubilization by Triton X-100 was determined from electron density calculations supported this hypothesis [35]. Accordingly, the headgroup separation across bilayers formed by DRM fractions, calculated

from Bragg reflections recorded from multilamellar structures, was found to be about 4.8 nm and similar to SM:Chol dispersions forming Lo phase. This was significantly greater than the corresponding distance in bilayers formed from detergent-soluble lipids which were invariably less than 4 nm. Accurate electron density calculations could not be performed on the multilamellar structures formed by erythrocyte rafts in the present study because the camera configuration only allowed the collection of two orders of the lamellar repeat. The present results, however, are in marked contrast to the model reported earlier [35] since the *d* spacings from multilamellar structures formed by erythrocyte rafts (6.1 nm) are significantly less than that reported for the model lipid rafts (7 nm) despite the presence of protein in the membrane raft preparation. Clearly the presence of surface protein may be a factor because differences in thickness of about 0.4 nm between Lo and L $\alpha$  phases have been reported in mixed lipid systems on the basis of atomic force microscopic measurements [55].

### Acknowledgments

The synchrotron X-ray diffraction experiments and freeze-fracture electron microscopic studies were ably assisted by Dr. Anthony Gleeson and Dr. Tony Brain, respectively.

### References

- [1] B.R. Lentz, M. Hoechli, Y. Barenholz, *Biochemistry* 20 (1981) 6803–6809.
- [2] J.H. Ipsen, G. Karlstrom, O.G. Mouritsen, H. Wennerstrom, M.J. Zuckermann, *Biochim. Biophys. Acta* 905 (1987) 162–172.
- [3] O.G. Mouritsen, *Chem. Phys. Lipids* 57 (1991) 179–194.
- [4] S.N. Ahmed, D.A. Brown, E. London, *Biochemistry* 36 (1997) 10944–10953.
- [5] M.S. Bretscher, S. Munro, *Science* 261 (1993) 1280–1281.
- [6] Q. Tang, M. Edidin, *Biophys. J.* 81 (2001) 196–203.
- [7] N. Foger, R. Marhaba, M. Zoller, *J. Cell Sci.* 114 (2001) 1169–1178.
- [8] L.A. Gheber, M. Edidin, *Biophys. J.* 77 (1999) 3163–3175.
- [9] E.B. Babiychuk, A. Draeger, *J. Cell Biol.* 150 (2000) 1113–1124.
- [10] S. Oliferenko, K. Paiha, T. Harder, V. Gerke, C. Schwarzler, H. Schwarz, H. Beug, U. Gunthert, L.A. Huber, *J. Cell Biol.* 146 (1999) 843–854.
- [11] A.K. Kenworthy, N. Petranova, M. Edidin, *Mol. Biol. Cell* 11 (2000) 1645–1655.
- [12] A.K. Kenworthy, M. Edidin, *J. Cell Biol.* 142 (1998) 69–84.
- [13] D.A. Brown, E. London, *J. Biol. Chem.* 275 (2000) 17221–17224.
- [14] T. Harder, P. Scheiffele, P. Verkade, K. Simons, *J. Cell Biol.* 141 (1998) 929–942.
- [15] K. Simons, E. Ikonen, *Nature* 387 (1997) 569–572.
- [16] K. Simons, E. Ikonen, *Science* 290 (2000) 1721–1726.
- [17] I. Gkantiragas, B. Brugger, E. Stuken, D. Kaloyanova, X.Y. Li, K. Lohr, F. Lottspeich, F.T. Wieland, J.B. Helms, *Mol. Biol. Cell.* 12 (2001) 1819–1833.
- [18] E.K. Fridriksson, P.A. Shipkova, E.D. Sheets, D. Holowka, B. Baird, F.W. McLafferty, *Biochemistry* 38 (1999) 8056–8063.
- [19] K. Hanada, M. Nishijima, Y. Akamatsu, R.E. Pagano, *J. Biol. Chem.* 270 (1995) 6254–6260.
- [20] F. Galbiati, B. Razani, M.P. Lisanti, *Cell* 106 (2001) 403–411.
- [21] S. Moffett, D.A. Brown, M.E. Linder, *J. Biol. Chem.* 275 (2000) 2191–2198.
- [22] A. Prinetti, V. Chigorno, G. Tettamanti, S. Sonnino, *J. Biol. Chem.* 275 (2000) 11658–11665.
- [23] W.B. Huttner, J. Zimmerberg, *Curr. Opin. Cell. Biol.* 13 (2001) 478–484.
- [24] T. Lang, D. Bruns, D. Wenzel, D. Riedel, P. Holroyd, C. Thiele, R. Jahn, *EMBO J.* 20 (2001) 2202–2213.
- [25] L.H. Chamberlain, R.D. Burgoyne, G.W. Gould, *Proc. Natl. Acad. Sci. USA* 98 (2001) 5619–5624.
- [26] B. Baird, E.D. Sheets, D. Holowka, *Biophys. Chem.* 82 (1999) 109–119.
- [27] D.A. Brown, E. London, *Annu. Rev. Cell Dev. Biol.* 14 (1998) 111–136.
- [28] K.A. Field, D. Holowka, B. Baird, *J. Biol. Chem.* 272 (1997) 4276–4280.
- [29] M. Kawabuchi, Y. Satomi, T. Takao, Y. Shimonishi, S. Nada, K. Nagai, A. Tarakhovskiy, M. Okada, *Nature* 404 (2000) 999–1003.
- [30] K.R. Solomon, E.A. Kurt-Jones, R.A. Saladino, A.M. Stack, I.F. Dunn, M. Ferretti, D. Golenbock, G.R. Fleisher, R.W. Finberg, *J. Clin. Invest.* 102 (1998) 2019–2027.
- [31] F. Lafont, P. Verkade, T. Galli, C. Wimmer, D. Louvard, K. Simons, *Proc. Natl. Acad. Sci. USA* 96 (1999) 3734–3738.
- [32] P. Scheiffele, M.G. Roth, K. Simons, *EMBO J.* 16 (1997) 5501–5508.
- [33] G.J. Schutz, G. Kada, V.P. Pastushenko, H. Schindler, *EMBO J.* 19 (2000) 892–901.
- [34] E.D. Sheets, G.M. Lee, R. Simson, K. Jacobson, *Biochemistry* 36 (1997) 12449–12458.
- [35] M. Gandhavadi, D. Allende, A. Vidal, S.A. Simon, T.J. McIntosh, *Biophys. J.* 82 (2002) 1469–1482.
- [36] T.T. Markovska, T.N. Neicheva, A.B. Momchilova-Pankova, K.S. Koumanov, R. Infante, *Int. J. Biochem.* 22 (1990) 1009–1013.
- [37] E.G. Bligh, W.J. Dyer, *Can. J. Med. Sci.* 37 (1959) 911–917.
- [38] M.N. Nikolova-Karakashian, H. Petkova, K.S. Koumanov, *Biochimie* 74 (1992) 153–159.
- [39] C. Boulin, R. Kempf, A. Gabriel, M.H.J. Koch, S.M. McLaughlin, *Nucl. Instrum. Methods A249* (1986) 399–409.
- [40] W. Folkhard, D. Christmann, W. Geercken, E. Knorz, M.H. Koch, E. Mosler, H. Nemetschek-Gansler, T. Nemetschek, *Z. Naturforsch. [C]* 42 (1987) 1303–1306.
- [41] J. Florin-Christensen, C.E. Suarez, M. Florin-Christensen, M. Wainzelbaum, W.C. Brown, T.F. McElwain, G.H. Palmer, *Proc. Natl. Acad. Sci. USA* 98 (2001) 7736–7741.
- [42] J. Florin-Christensen, C.E. Suarez, M. Florin-Christensen, S.A. Hines, T.F. McElwain, G.H. Palmer, *Mol. Biochem. Parasitol.* 106 (2000) 147–156.
- [43] D. Bach, E. Wachtel, *Biochim. Biophys. Acta* 1610 (2003) 187–197.
- [44] H.M. McConnell, A. Radhakrishnan, *Biochim. Biophys. Acta* 1610 (2003) 159–173.
- [45] H.M. McConnell, M. Vrljic, *Annu. Rev. Biophys. Biomol. Struct.* 32 (2003) 469–492.
- [46] G. Kellner-Weibel, P.G. Yancey, W.G. Jerome, T. Walser, R.P. Mason, M.C. Phillips, G.H. Rothblat, *Arterioscler. Thromb. Vasc. Biol.* 19 (1999) 1891–1898.
- [47] X.M. Li, M.M. Momsen, H.L. Brockman, R.E. Brown, *Biophys. J.* 85 (2003) 3788–3801.
- [48] R.F. de Almeida, A. Fedorov, M. Prieto, *Biophys. J.* 85 (2003) 2406–2416.
- [49] A.J. Costa-Filho, Y. Shimoyama, J.H. Freed, *Biophys. J.* 84 (2003) 2619–2633.
- [50] E.J. Smart, Y.S. Ying, C. Mineo, R.G. Anderson, *Proc. Natl. Acad. Sci. USA* 92 (1995) 10104–10108.



- [51] L.J. Pike, X. Han, K.N. Chung, R.W. Gross, *Biochemistry* 41 (2002) 2075–2088.
- [52] D. Furtado, W.P. Williams, A.P. Brain, P.J. Quinn, *Biochim. Biophys. Acta* 555 (1979) 352–357.
- [53] H. Heerklotz, *Biophys. J* 83 (2002) 2693–2701.
- [54] S. Munro, *EMBO J.* 14 (1995) 4695–4704.
- [55] H.A. Rinia, J.W. Boots, D.T. Rijkers, R.A. Kik, M.M. Snel, R.A. Demel, J.A. Killian, J.P. van der Eerden, B. de Kruijff, *Biochemistry* 41 (2002) 2814–2824.